

Supplementary Material

Study of the versatility of CuBTC@IL derived materials for heterogeneous catalysis

Edurne S. Larrea,^{*a,b} Roberto Fernández de Luis,^c Arkaitz Fidalgo-Marijuan,^{a,c} Eva M. Maya,^d Marta Iglesias^d and María I. Arriortua^{a,c}

^aDpto. Mineralogía y Petrología, Universidad del País Vasco, UPV/EHU, Sarriena s/n, 48940 Leioa, Spain; ^bLe Studium Research Fellow, Loire Valley Institute for Advanced Studies, Orléans & Tours, France; ^cBCMaterials (Basque Center for Materials, Applications & Nanostructures), UPV/EHU Scientific Park, Martina Casiano Building, 3th floor, Sarriena s/n, Leioa; ^dInstituto de Ciencia de Materiales de Madrid-CSIC, Sor Juana Inés de la Cruz 3, Cantoblanco, 28049, Madrid, Spain.

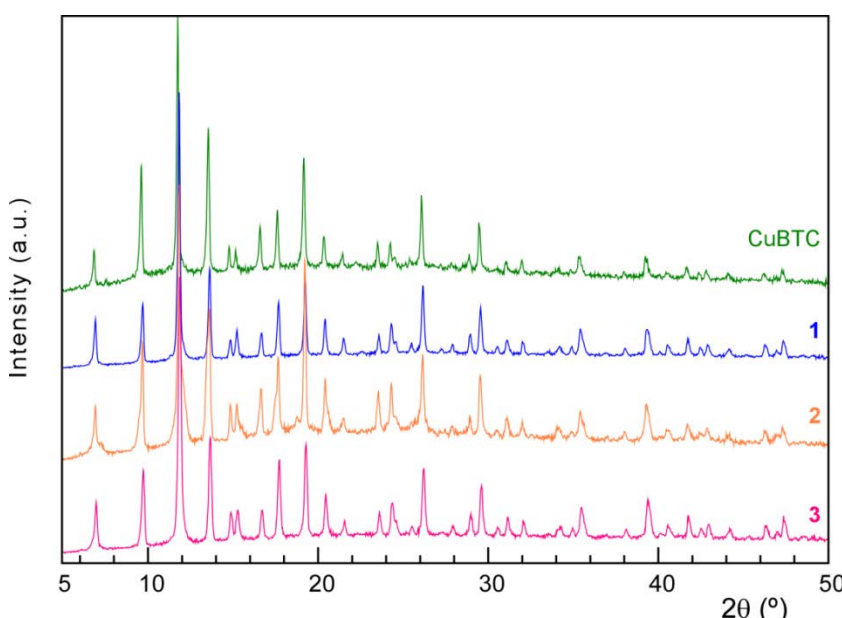


Figure S.1. Diffraction patterns of CuBTC (Basolite® C300), **1**, **2** and **3**.

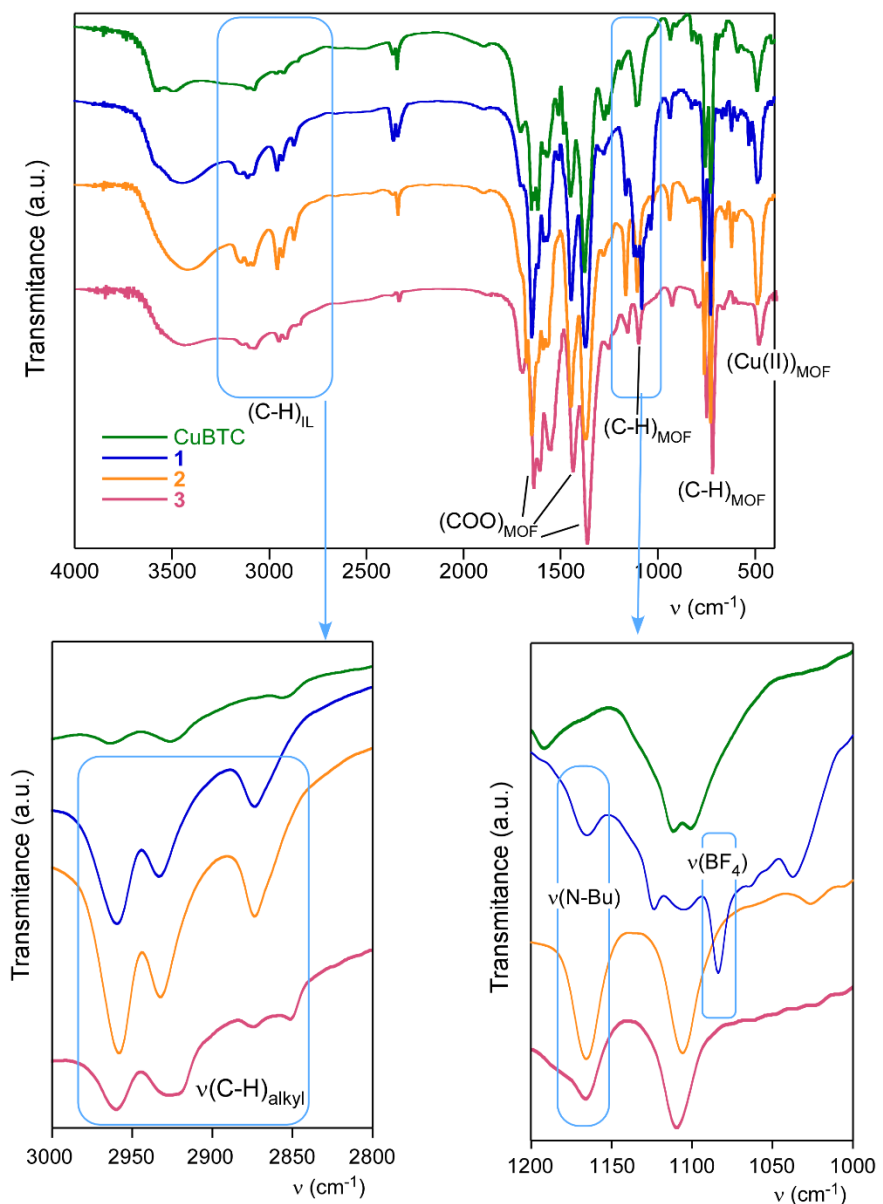


Figure S.2. FT-IR spectra of CuBTC (Basolite® C300), **1**, **2** and **3**.

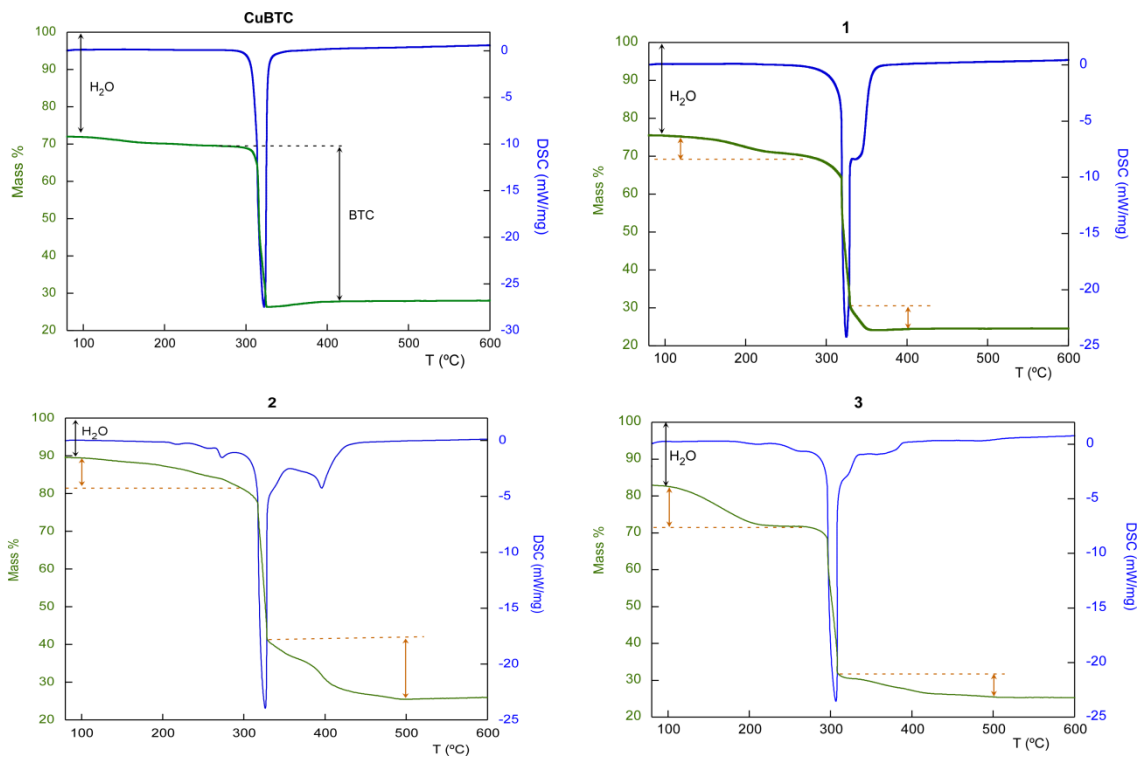


Figure S.3. Thermogravimetric (green line) and DSC (blueline) curves of CuBTC (Basolite® C300), **1**, **2** and **3**. Extra weight loss stages for IL loaded materials are marked in orange.

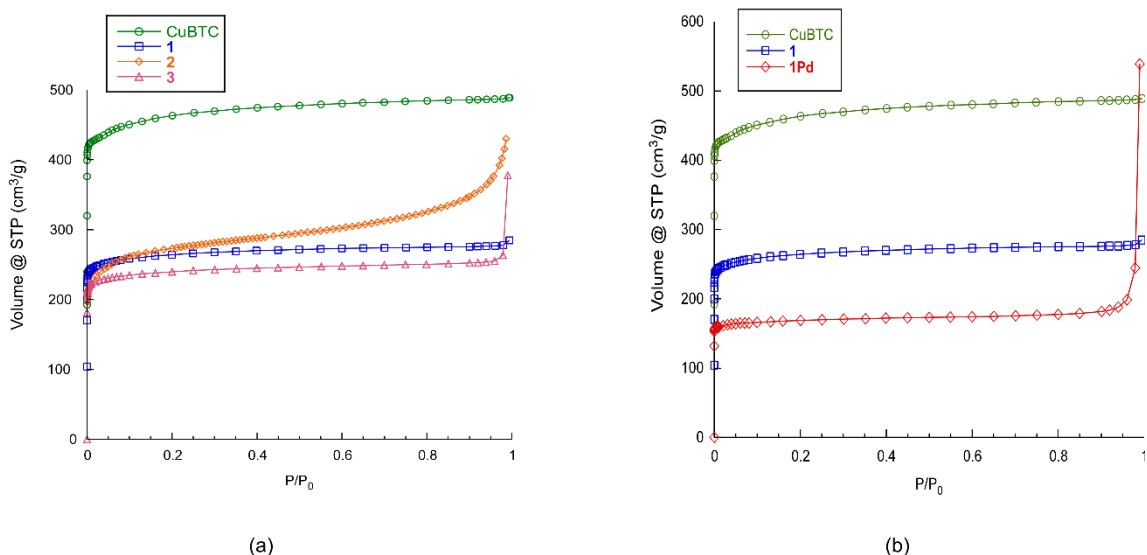


Figure S.4. N_2 isotherms at 77 K for CuBTC (Basolite® C300) and functionalized materials (a) **1**, **2** and **3**, and (b) **1** and **1Pd**.

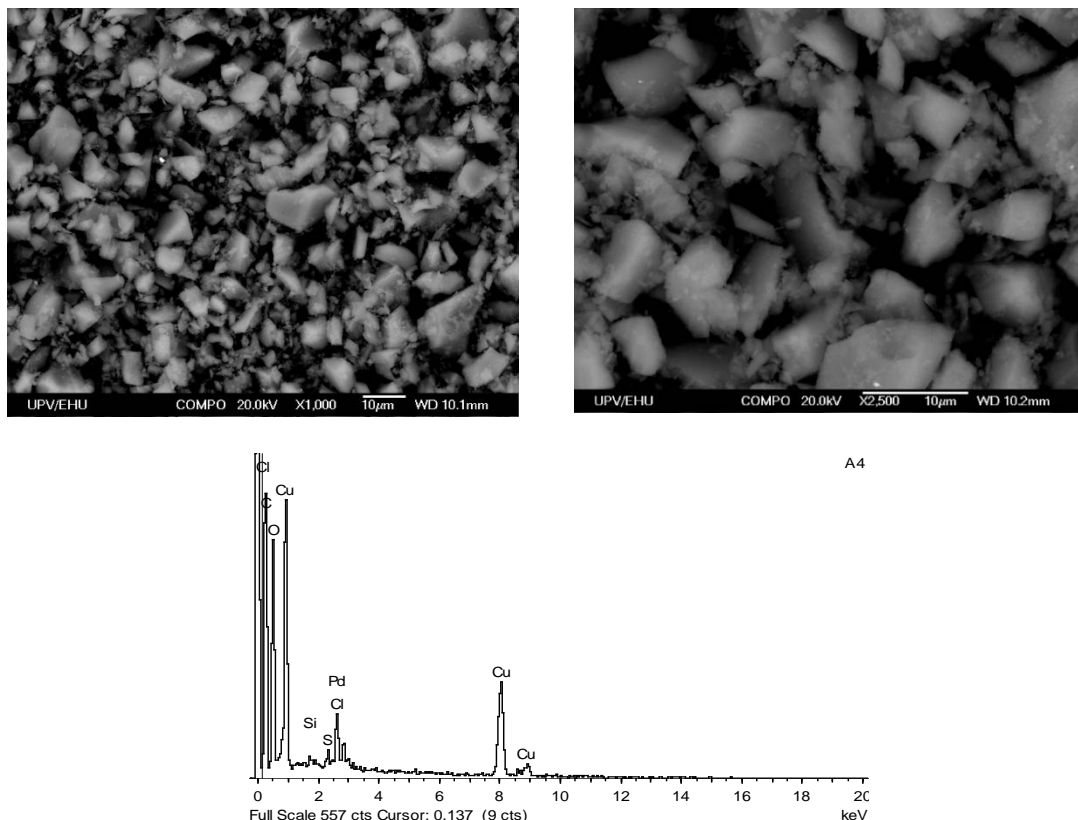


Figure S.5. SEM micrographs of **1Pd** and EDX punctual analysis of one particle.

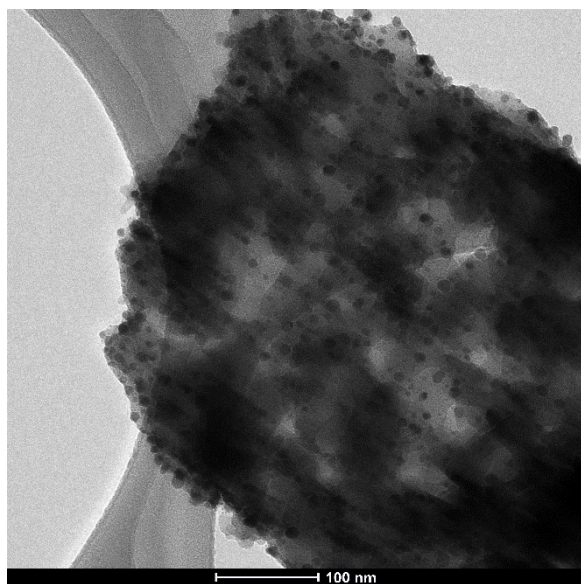


Figure S.6. TEM micrograph of **1Pd**.

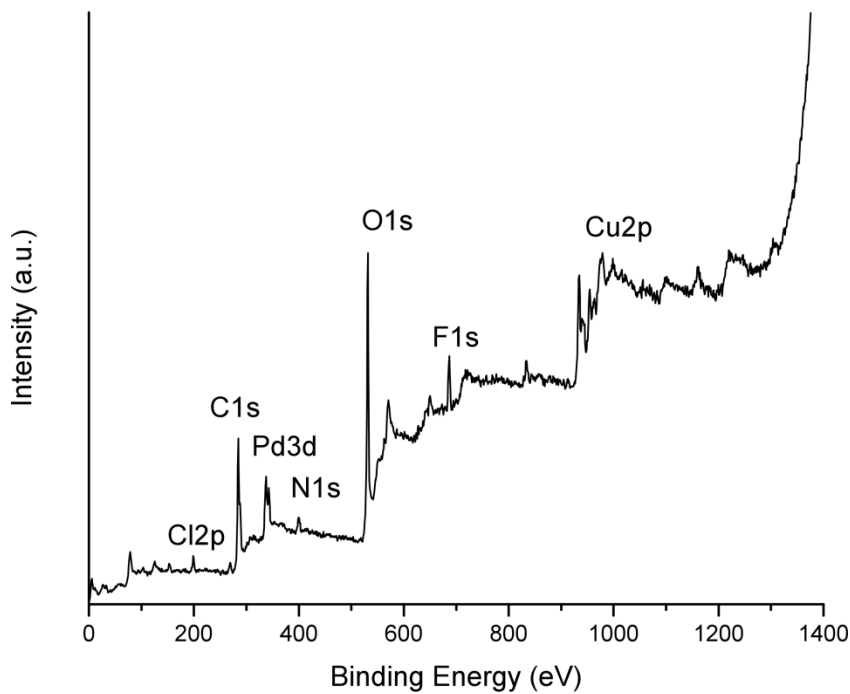


Figure S.7. XPS survey spectra of **1Pd**.

Table S.1. Results of the deconvolution of the high resolution XPS spectra for each element for **1Pd**.

Element	Peak	Position	FWHM	R.S.F.	Area	% Conc.	% Atomic rel. conc.
C	C-C, C-H	284.6	2.583	1	6426	35.257	49.0
	O-C=O	288.3	2.583	1	2504	13.739	
O	O 1s	531.3	3.375	2.93	16269.5	30.466	30.5
Pd	Pd (3d 5/2)	336.3	2.416	16	1417.1	0.486	2.1
	Pd (3d 3/2)	341.5	2.416	16	950.5	0.326	
	Pd (3d 5/2)	338.3	2.416	16	2275.6	0.78	
	Pd (3d 3/2)	343.5	2.416	16	1526.3	0.523	
Cu	Cu 2p 3/2 (2+)	934.4	3.784	16.7	8454	2.778	4.5
	Cu 2p 3/2 (2+, sat)	940.4	3.623	16.7	2623.1	0.862	
	Cu 2p 3/2 (2+, sat)	943.8	3.623	16.7	2615.6	0.859	
F	F 1s	686.9	3.416	4.43	4524.7	5.604	5.6
N	N 1s	400.0	3.618	1.8	1163.4	3.546	3.5
Cl	Cl (2p 3/2)	199.1	2.481	2.29	600.4	1.439	2.2
	Cl (2p 1/2)	200.9	2.481	2.29	300.3	0.719	
Si*	Si 2p	103.0	2.916	0.817	389.4	2.615	2.6

*Near to the noise, estimation

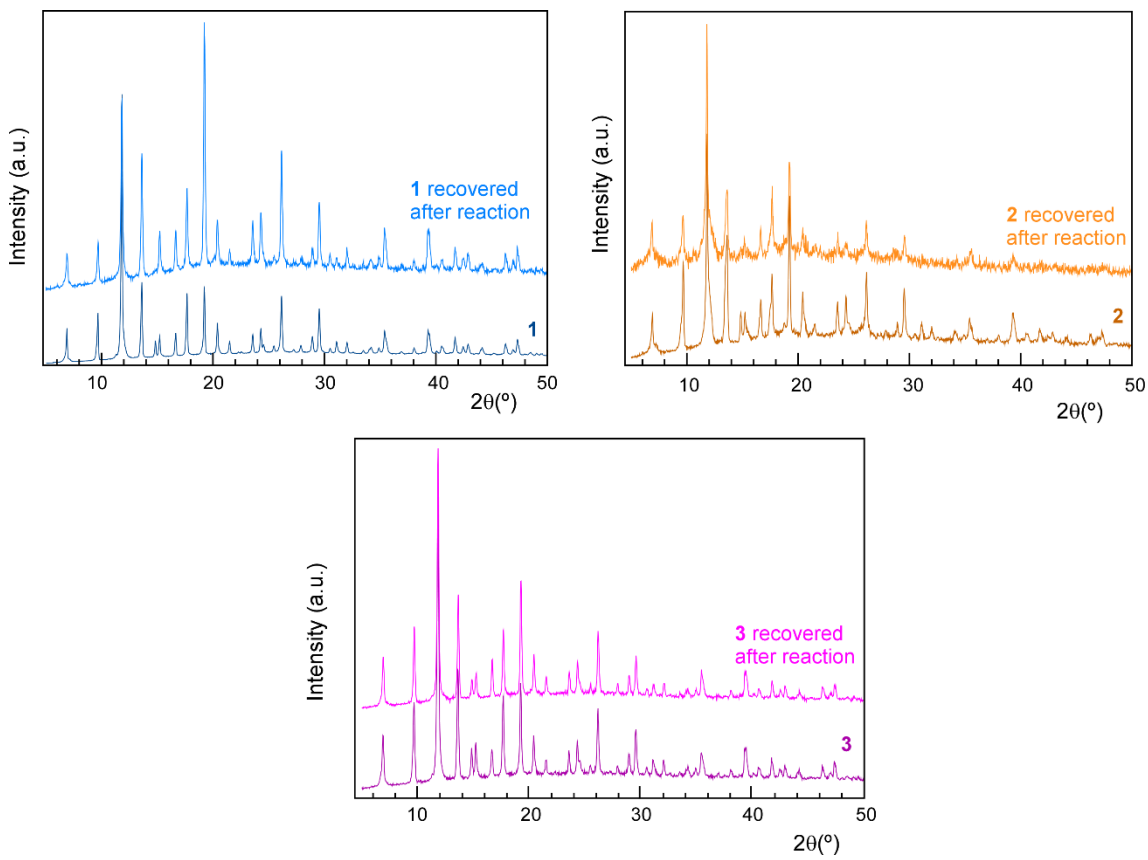


Figure S.8. X-ray diffraction patterns of catalysts **1**, **2** and **3** before and after the cycloaddition of CO_2 to epoxides.

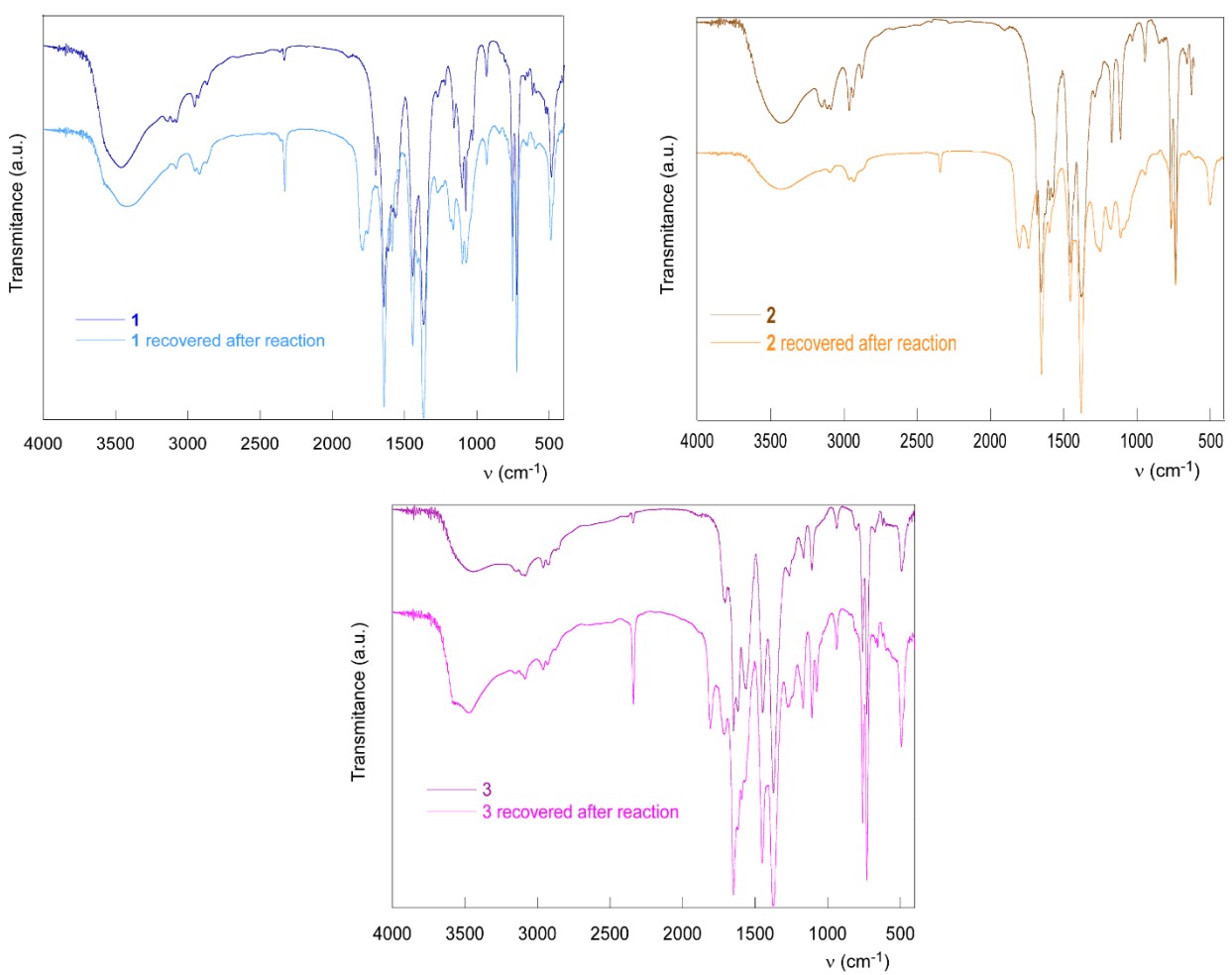


Figure S.9. FT-IR spectra of catalysts **1**, **2** and **3** before and after the cycloaddition of CO_2 to epoxides.

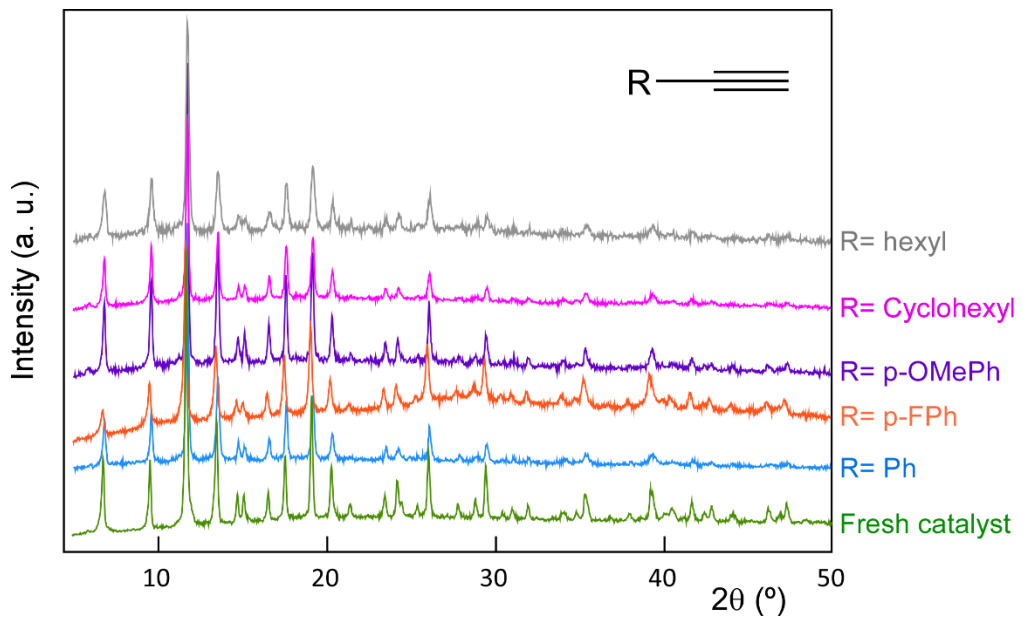


Figure S.10. X-ray diffraction patterns of the recovered catalyst **1Pd** after the reaction with different alkynes.

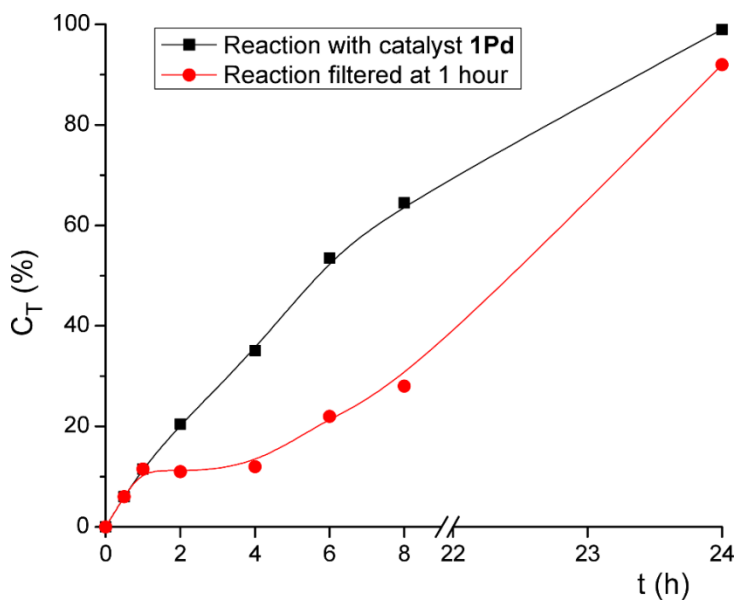


Figure S.11. Kinetic profiles of the homocoupling reaction of ethynilbenzene with catalyst **1Pd** and after hot filtration.

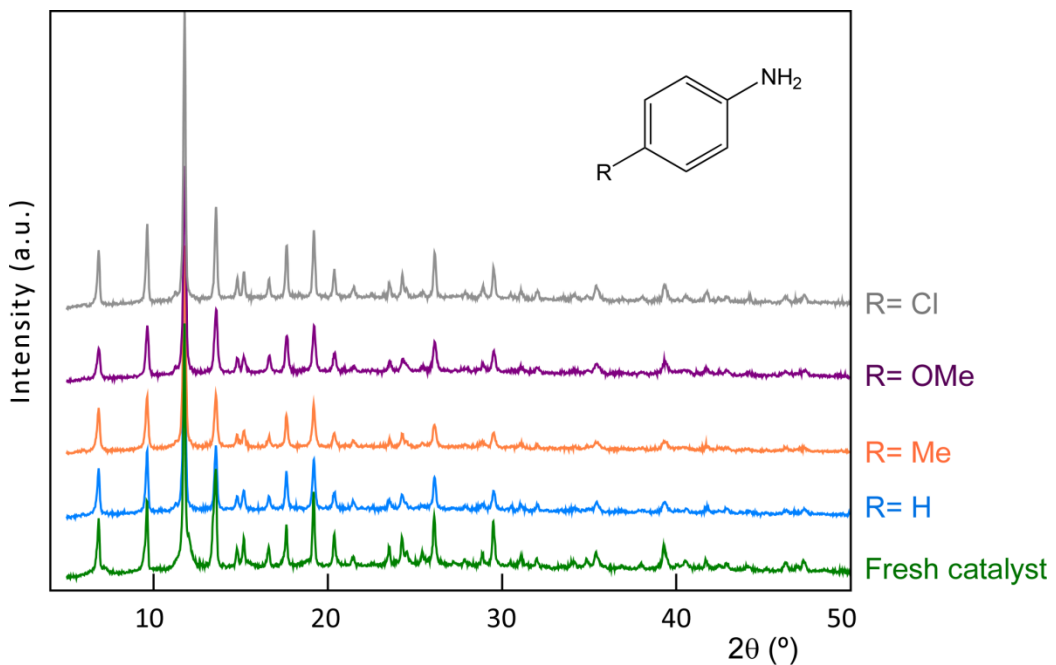


Figure S.12. X-ray diffraction patterns of the recovered catalyst **1Pd** after the reaction with different amines.

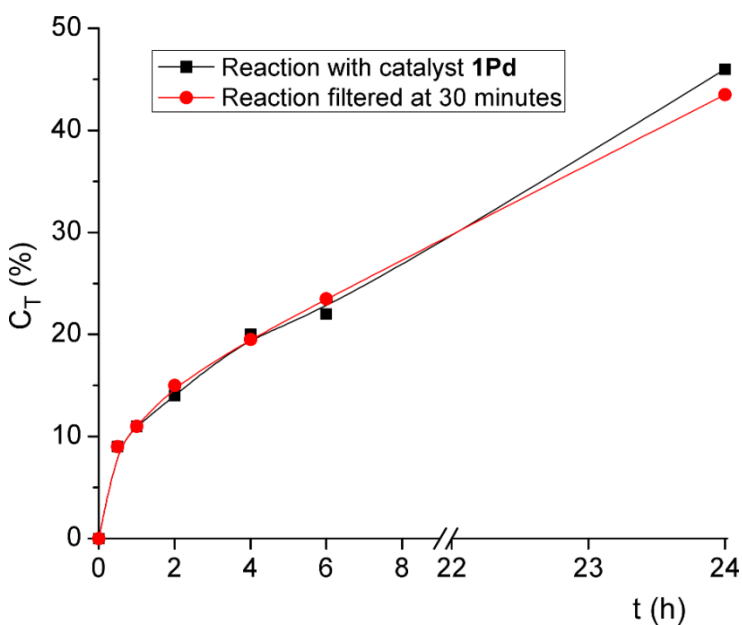


Figure S.13. Kinetic profiles of the aniline alkylation with benzyl alcohol with catalyst **1Pd** and after hot filtration.